Journal of Sound and Vibration (1997) **199**(4), 679–696

NON-LINER VIBRATIONS OF A BEAM–MASS SYSTEM UNDER DIFFERENT BOUNDARY CONDITIONS

E. Özkaya, M. Pakdemirli and H. R. Öz

Department of Mechanical Engineering, Celal Bayar University, 45040 Manisa, Turkey

(*Received* 17 *January* 1996, *and in final form* 3 *July* 1996)

An Euler–Bernoulli beam and a concentrated mass on this beam are considered as a beam–mass system. The beam is supported by immovable end conditions, thus leading to stretching during the vibrations. This stretching produces cubic non-linearities in the equations. Forcing and damping terms are added into the equations. The dimensionless equations are solved for five different set of boundary conditions. Approximate solutions of the equations are obtained by using the method of multiple scales, a perturbation technique. The first terms of the perturbation series lead to the linear problem. Natural frequencies and mode shapes for the linear problem are calculated exactly for different end conditions. Second order non-linear terms of the perturbation series appear as corrections to the linear problem. Amplitude and phase modulation equations are obtained. Non-linear free and forced vibrations are investigated in detail. The effects of the position and magnitude of the mass, as well as effects of different end conditions on the vibrations, are determined.

1. INTRODUCTION

Beam–mass systems are frequently used as design models in engineering. Approximate and exact analyses have been carried out for calculating the natural frequencies of a beam–mass system under various end conditions [1–8]. When the amplitudes of vibrations are not small, a non-linear analysis becomes inevitable. The non-linearities may be inserted in different ways. In particular, in the case of immovable end conditions, non-linearities arise due to the axial stretching of the beam during the vibrations. Woinowsky-Krieger [9] and Burgreen [10] were the first to study the effects of axial stretching on the vibrations of beams. Srinivasan [11] applied the Ritz–Galerkin technique to analyze the large amplitude free oscillations of beams and plates with stretching. In addition to stretching, Wrenn and Mayers [12] included the effects of transverse shear and rotary inertia. The work on non-linear beam vibrations up to 1979 has been reviewed by Nayfeh and Mook [13]. Hou and Yuan [14] investigated the design sensitivity of a stretched beam with immovable ends. McDonald [15] investigated the dynamic mode couplings of a hinged beam with uniformly distributed loading. Dokainish and Kumar [16] treated a cantilever beam with a tip mass supported by a non-linear spring. Finally, Pakdemirli and Nayfeh [17] studied the non-linear vibrations of a beam–spring–mass system. The sources of the non-linearities include stretching and a non-linear spring supporting the mass.

In this study, we extend the analysis of reference [17] by considering five different set of boundary conditions. However, we do not include the effects of a non-linear spring, so that we can analyze the effect of stretching with ease. The different boundary conditions, and the location and the magnitude of the mass are the control parameters for our problem.

0022–460X/97/040679 + 18 $25.00/0/sv960663

The method of multiple scales, a perturbation technique, is used to solve the non-linear equations approximately. The first terms in the expansions lead to the linear problem. The natural frequencies and mode shapes are calculated exactly and tabulated for different end conditions, locations of mass and mass ratios. The addition of non-linear terms, then, introduces corrections to the linear problem. The amplitude and phase modulation equations are determined from the non-linear analysis. Free vibrations and forced vibrations with damping are investigated in detail. The effects of mid-plane stretching on the beam vibrations are studied for different control parameters.

2. EQUATIONS OF MOTION

The system considered is a beam with a concentrated mass located at $x = x_s$, where x is the spatial co-ordinate along the beam length. Five different cases of support at the ends of the beam are treated, as shown in Figure 1.

The Lagrangian for the system can be written as

$$\mathscr{L} = (1/2)\int_0^{x_s} \rho A \dot{w}_1^{*2}\,\mathrm{d}x^* + (1/2)\int_{x_s}^{L} \rho A \dot{w}_2^{*2}\,\mathrm{d}x^* + (1/2)M\dot{w}_1^{*2}(x_s, t^*)$$

$$- (1/2)\int_0^{x_s} EIw_1''^{*2}\,\mathrm{d}x^* - (1/2)\int_{x_s}^{L} EIw_2''^{*2}\,\mathrm{d}x^*$$

$$- (1/2)\int_0^{x_s} EA(u_1'^{*} + 1/2w_1'^{*2})^2\,\mathrm{d}x^* - (1/2)\int_{x_s}^{L} EA(u_2'^{*2} + 1/2w'^{*2})^2\,\mathrm{d}x^*, \qquad (1)$$

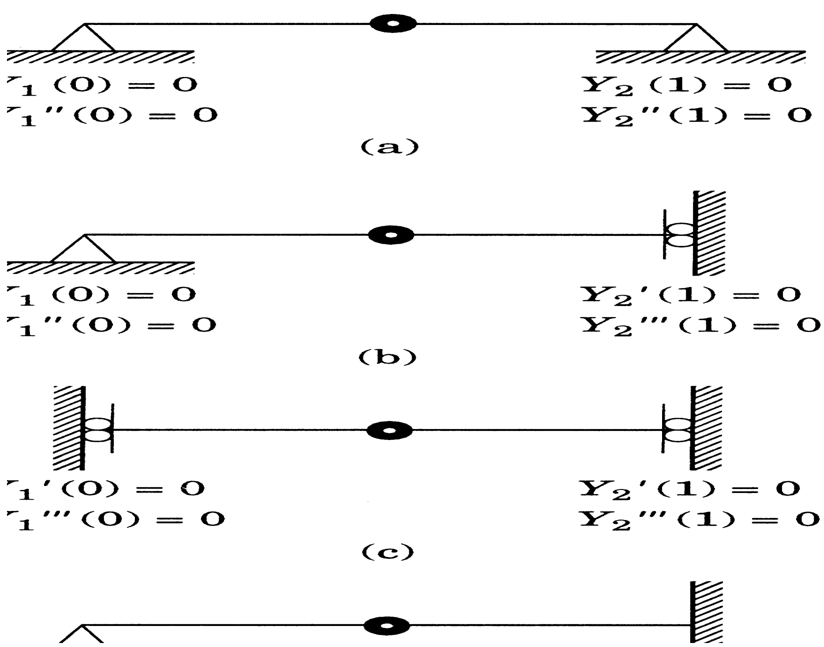

Figure 1. The support end conditions for five different cases. (a) Case I; (b) Case II; (c) Case III; (d) Case IV; (e) Case V.

where L is the length, ρ is the density, A is the cross-sectional area, E is Young's modulus, I is the moment of inertia of the beam cross-section with respect to the neutral axis of the beam, u_1 and u_2 are the left and right axial displacements and w_1 and w_2 are the left and right transverse displacements with respect to the concentrated mass M. $(\dot{})$ denotes differentiation with respect to time t^* and $(\,)'$ denotes differentiation with respect to the spatial variable x^*. The first three terms in equation (1) are the kinetic energies of the beam and concentrated mass, the following two terms are the potential energies due to bending and the last two terms are the potential energies due to stretching of the beam.

Invoking Hamilton's principle,

$$\delta \int_{t_1}^{t_2} \mathscr{L}\,\mathrm{d}t^* = 0 \tag{2}$$

and substituting the Lagrangian from equation (1), performing the necessary algebra and eliminating the axial displacements [17], one finally obtains the following non-linear coupled integro-differential equations:

$$\rho A\ddot{w}_1^* + EIw_1^{iv*} = \frac{EA}{2L}\left[\int_0^{x_s} w_1'^{*2}\,\mathrm{d}x^* + \int_{x_s}^{L} w_2'^{*2}\,\mathrm{d}x^*\right]w_1''^* - \mu^*\dot{w}_1^* + F_1^*\cos\Omega^* t^*, \tag{3}$$

$$\rho A\ddot{w}_2^* + EIw_2^{iv*} = \frac{EA}{2L}\left[\int_0^{x_s} w_1'^{*2}\,\mathrm{d}x^* + \int_{x_s}^{L} w_2'^{*2}\,\mathrm{d}x^*\right]w_2''^* - \mu^*\dot{w}_2^* + F_2^*\cos\Omega^* t^*. \tag{4}$$

Note that viscous damping with damping coefficient μ^*, and external excitation with amplitude F_i^* and frequency Ω^* are added to the equations. The boundary conditions at the ends are given in Figure 1 for each case. The boundary conditions at the location of the concentrated mass, which apply to all cases, are as follows:

$$w_1^*(x_s, t^*) = w_2^*(x_s, t^*), \qquad w_1'^*(x_s, t^*) = w_2'^*(x_s, t^*), \qquad w_1''^*(x_s, t^*) = w_2''^*(x_s, t^*), \tag{5}$$

$$EIw_1'''^*(x_s, t^*) - EIw_2'''^*(x_s, t^*) - M\ddot{w}_1^*(x_s, t^*) = 0. \tag{6}$$

The equations are made dimensionless though the definitions

$$x = x^*/L, \qquad w_{1,2} = w_{1,2}^*/r, \qquad \eta = x_s/L, \qquad t = (1/L^2)(EI/\rho A)^{1/2} t^*,$$

$$\alpha = M/\rho AL, \qquad \Omega = \Omega^* L^2/(EI/\rho A)^{1/2}, \qquad \bar{F}_{1,2} = F_{1,2}^*/EIr, \qquad 2\bar{\mu} = (\mu^* L^2)/(\rho AEI)^{1/2}, \tag{7}$$

which, upon substituting into the original equations, yield

$$\ddot{w}_1 + w_1^{iv} = (1/2)\left[\int_0^{\eta} w_1'^2\,\mathrm{d}x + \int_{\eta}^{1} w_2'^2\,\mathrm{d}x\right]w_1'' - 2\bar{\mu}\dot{w}_1 + \bar{F}_1\cos\Omega t, \tag{8}$$

$$\ddot{w}_2 + w_2^{iv} = (1/2)\left[\int_0^{\eta} w_1'^2\,\mathrm{d}x + \int_{\eta}^{1} w_2'^2\,\mathrm{d}x\right]w_2'' - 2\bar{\mu}\dot{w}_2 + \bar{F}_2\cos\Omega t, \tag{9}$$

$$w_1(\eta, t) = w_2(\eta, t), \qquad w_1'(\eta, t) = w_2'(\eta, t), \qquad w_1''(\eta, t) = w_2''(\eta, t), \tag{10}$$

$$w_1'''(\eta, t) - w_2'''(\eta, t) - \alpha\ddot{w}_1(\eta, t) = 0. \tag{11}$$

TABLE 1

Mode shapes and transcendental frequency equations for different end conditions

	Mode shapes	Transcendental frequency equations
Case I 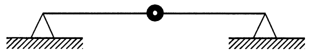 (a)	$Y_1(x) = C\{\tanh\beta(\cot\beta\sin\beta\eta - \cos\beta\eta)\sin\beta x$ $+ (\tanh\beta\cosh\beta\eta - \sinh\beta\eta)\sinh\beta x\}$, $Y_2(x) = C\{\tanh\beta\sin\beta\eta(\cot\beta\sin\beta x - \cos\beta x) + \sinh\beta\eta$ $\times(\tanh\beta\cosh\beta x - \sinh\beta x)\}$	$2\tanh\beta\tan\beta + \alpha\beta\{\tanh\beta\sin\beta\eta$ $\times(\sin\beta\eta - \tan\beta\cos\beta\eta)$ $+ \tan\beta\sinh\beta\eta(\tanh\beta\cosh\beta\eta - \sinh\beta\eta)\} = 0$
Case II 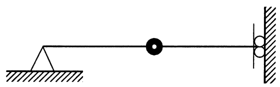 (b)	$Y_1(x) = C\{(\cot\beta\cot\beta\eta + 1)\sin\beta x - \sinh\beta\eta\cot\beta\,\mathrm{cosec}\,\beta\eta$ $\times(\coth\beta\eta - \tanh\beta)\sinh\beta x\}$, $Y_2(x) = C\{\cot\beta\cos\beta x + \sin\beta x - \sinh\beta\eta\cot\beta\,\mathrm{cosec}\,\beta\eta$ $\times(\cosh\beta x - \tanh\beta\sinh\beta x)\}$	$2\cos\beta - \alpha\beta\{\cos\beta\cos\beta\eta\sin\beta\eta + \sin\beta\sin^2\beta\eta$ $- \sinh\beta\eta\cos\beta(\cosh\beta\eta - \tanh\beta\sinh\beta\eta)\} = 0$
Case III 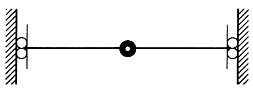 (c)	$Y_1(x) = C\{(\cos\beta(1-\eta)\sinh\beta\cos\beta x + \sin\beta\cosh\beta\,(1-\eta)$ $\cosh\beta x)\}$, $Y_2(x) = C\{(\cos\beta\eta\sinh\beta(\cos\beta\cos\beta x + \sin\beta\sin\beta x)$ $+ \sin\beta\cosh\beta\eta(\cosh\beta\cosh\beta x - \sinh\beta\sinh\beta x)\}$	$2\sin\beta\sinh\beta + \alpha\beta\{\cos\beta(1-\eta)\sinh\beta\cos\beta\eta$ $+ \sin\beta\cosh\beta(1-\eta)\cosh\beta\eta\} = 0$
Case IV 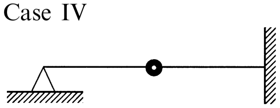 (d)	$Y_1(x) = C\{\{\sin\beta(1-\eta)\cosh\beta - \cos\beta(1-\eta)\sinh\beta$ $+ \sinh\beta\eta\}\sin\beta x + \{\sin\beta\eta - \sin\beta\cosh\beta(1-\eta)$ $+ \cos\beta\sinh\beta(1-\eta)\}\sinh\beta x\}$, $Y_2(x) = C\{\sin\beta\eta(\sin\beta\cosh\beta - \cos\beta\sinh\beta)\cos\beta x$ $+ \{\sinh\beta\eta - (\cos\beta\cosh\beta + \sin\beta\sinh\beta)\sin\beta\eta\}\sin\beta x$ $+ \{-\sinh\beta\eta(\sin\beta\cosh\beta - \cos\beta\sinh\beta)\}\cosh\beta x$ $+ \{\sin\beta\eta + \sinh\beta\eta(\sin\beta\sinh\beta - \cos\beta\cosh\beta)\}\sinh\beta x\}$	$2(\sinh\beta\cos\beta - \cosh\beta\sin\beta) + \alpha\beta\{\cosh\beta\eta\sinh\beta\eta$ $- \cos\beta\eta\sin\beta\eta)(\cos\beta\sinh\beta - \sin\beta\cosh\beta)$ $- \sin^2\beta\eta(\sinh\beta\sin\beta + \cosh\beta\cos\beta)$ $- \sinh^2\beta\eta(\cosh\beta\cos\beta - \sinh\beta\sin\beta)$ $+ 2\sinh\beta\eta\sin\beta\eta\} = 0$
Case V 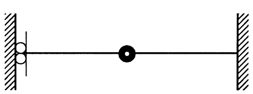 (e)	$Y_1(x) = C\{\{\cosh\beta\eta + \sin\beta(1-\eta)\sinh\beta - \cos\beta(1-\eta)\cosh\beta\}$ $\cos\beta x + \{\cos\beta\eta - \cos\beta\cosh\beta(1-\eta)$ $- \sin\beta\sinh\beta(1-\eta)\}\cosh\beta x\}$, $Y_2(x) = C\{\{\cosh\beta\eta + (\sin\beta\sinh\beta - \cos\beta\cosh\beta)\mathit{cos}\ \beta\eta\}\cos\beta x$ $- \{(\cos\beta\sinh\beta + \sin\beta\cosh\beta)\cos\beta\eta\}\sin\beta x$ $+ \{\cos\beta\eta - \cosh\beta\eta\,(\cos\beta\cosh\beta + \sin\beta\sinh\beta)\}$ $\times\cosh\beta x + \{\cosh\beta\eta(\cos\beta\sinh\beta + \sin\beta\cosh\beta)\}\sinh\beta x\}$	$2(\cos\beta\sinh\beta + \sin\beta\cosh\beta) - \alpha\beta\{2\cos\beta\eta\cosh\beta\eta$ $+ (\cos\beta\sinh\beta + \sin\beta\cosh\beta)(\sinh\beta\eta\cosh\beta\eta$ $- \cos\beta\eta\sin\beta\eta) + \sin\beta\sinh\beta$ $\times(\cos^2\beta\eta - \cosh^2\beta\eta) - \cos\beta\cosh\beta$ $\times(\cos^2\beta\eta + \cosh^2\beta\eta)\}$

The end conditions are as in Figure 1, except that all t^* will be replaced by t, all L by 1 and w^* by w. The term r in equations (7) is the radius of gyration of the beam cross-section and α is the ratio of the concentrated mass to the beam mass.

3. APPROXIMATE ANALYTICAL SOLUTIONS

In this section, we search for the approximate solutions of equations (8) and (9) with the associated boundary conditions. We apply the method of multiple scales (a perturbation technique) [13, 18] to the partial differential system and boundary conditions irectly. This direct treatment of partial differential systems (the direct perturbation method) has some advantages over the more common method of discretizing the partial differential system and then applying perturbations (the discretization perturbation method) [19]. In our case, however, both methods would yield identical results, since we are not considering a higher order perturbation scheme.

Due to the absence of quadratic non-linearities, we assume expansions of the forms

$$w_1(x, t; \epsilon) = \epsilon w_{11}(x, T_0, T_2) + \epsilon^3 w_{13}(x, T_0, T_2) + \dots, \tag{12}$$

$$w_2(x, t; \epsilon) = \epsilon w_{21}(x, T_0, T_2) + \epsilon^3 w_{23}(x, T_0, T_2) + \dots, \tag{13}$$

where ϵ is a small book-keeping parameter artifically inserted into the equations. This parameter can be taken as 1 at the end upon keeping in mind, however, that deflections are small. We therefore investigate a weakly non-linear system. $T_0 = t$ is the fast time scale, whereas $T_2 = \epsilon^2 t$ is the slow time scale. We consider only the primary resonance case and hence, the forcing and damping terms are ordered so that they counter the effect of non-linear terms: that is,

$$\bar{\mu} = \epsilon^2 \mu, \qquad \bar{F}_{1,2} = \epsilon^3 F_{1,2}. \tag{14}$$

The time derivatives are written as

$$(\dot{\ }) = D_0 + \epsilon^2 D_2, \qquad (\ddot{\ }) = D_0^2 + 2\epsilon^2 D_0 D_2, \qquad D_n = \partial/\partial T_n. \tag{15}$$

In reference [20], the equations governing the vibrations of a uniform beam with stretching and without a concentrated mass were solved by using a version of the Lindstedt–Poincaré technique. In this technique, periodic steady state solutions are assumed *a priori*, whereas in the method of multiple scales the periodic solutions as well as the transient solutions can be retrieved. As can be seen from our analysis, the expansion of the integral term (T in equation (4b) [20]) is unnecessary.

Inserting equation (12)–(15) into equation (8)–(11) and equating coefficients of like powers of ϵ, one obtains, to order ϵ,

$$D_0^2 w_{11} + w_{11}^{iv} = 0, \qquad D_0^2 w_{21} + w_{21}^{iv} = 0, \tag{16, 17}$$

$$w_{11} = w_{21}, \quad w_{11}' = w_{21}', \quad w_{11}'' = w_{21}'', \quad w_{11}''' - w_{21}''' - \alpha D_0^2 w_{11} = 0 \qquad \text{at } x = \eta, \tag{18}$$

$$w_{11} = w_{11}'' = 0 \quad \text{at } x = 0, \qquad w_{21} = w_{21}'' = 0 \quad \text{at } x = 1, \tag{19}$$

and, to order ϵ^3,

$$D_0^2 w_{13} + w_{13}^{iv} = -2D_0 D_2 w_{11} - 2\mu D_0 w_{11} + (1/2)\left[\int_0^\eta w_{11}'^2 \, dx + \int_\eta^1 w_{21}'^2 \, dx\right] w_{11}'' + F_1 \cos \Omega T_0, \tag{20}$$

$$D_0^2 w_{23} + w_{23}^{iv} = -2D_0 D_2 w_{21} - 2\mu D_0 w_{21} + (1/2)\left[\int_0^\eta w_{11}'^2\,dx + \int_\eta^1 w_{21}'^2\,dx\right] w_{21}'' + F_2 \cos \Omega T_0, \tag{21}$$

$$w_{13} = w_{23}, \quad w_{13}' = w_{23}', \quad w_{13}'' = w_{23}'', \quad w_{13}''' - w_{23}''' - \alpha D_0^2 w_{13} - 2\alpha D_0 D_2 w_{11} = 0 \qquad \text{at } x = \eta, \tag{22}$$

$$w_{13} = w_{13}'' = 0 \quad \text{at } x = 0, \qquad w_{23} = w_{23}'' = 0 \quad \text{at } x = 1. \tag{23}$$

Equations (19) and (23) are the boundary conditions corresponding to Case I. Boundary conditions for other cases can be written in a similar way.

3.1. LINEAR PROBLEM

The problem at order ϵ is linear. We assume a solution of the form

$$w_{11} = [A(T_2)\,e^{i\omega T_0} + cc]\,Y_1(x), \qquad w_{21} = [A(T_2)\,e^{i\omega T_0} + cc]\,Y_2(x), \tag{24, 25}$$

where cc represents the complex conjugate of the preceding terms. Substituting equations (24) and (25) into equations (16)–(19), one has

$$Y_1^{iv} - \omega^2 Y_1 = 0, \qquad Y_2^{iv} - \omega^2 Y_2 = 0, \tag{26, 27}$$

$$Y_1(\eta) = Y_2(\eta), \qquad Y_1'(\eta) = Y_2'(\eta), \qquad Y_1''(\eta) = Y_2''(\eta), \tag{28}$$

$$Y_1'''(\eta) - Y_2'''(\eta) + \alpha\omega^2 Y_1(\eta) = 0. \tag{29}$$

The end conditions for the Y_i functions are given in Table 1 for each case. Solving equations (26)–(29) exactly for different end conditions yields the mode shapes Y_i and natural frequencies ω. The mode shapes and transcendental frequency equations are listed in Table 1, where

$$\beta = \sqrt{\omega}. \tag{30}$$

The transcendental equations were numerically solved for the first five modes. Results are given in Table 2 for the different supporting conditions. For each case, the natural frequencies are listed for different α (the ratio of the concentrated mass to the beam mass) and η (the mass location parameter). Due to the symmetry in Cases I and III, results are given up to $\eta = 0{\cdot}5$.

3.2. NON-LINEAR PROBLEM

Because the homogeneous equations (16)–(19) have a non-trivial solution, the non-homogeneous problem (20)–(23) will have a solution only if a solvability condition is satisfied [13, 18]. To determine this condition, we first separate the secular and nonsecular terms by assuming a solution of the form

$$w_{13} = \phi_1(x, T_2)\,e^{i\omega T_0} + W_1(x, T_0, T_2) + cc, \tag{31}$$

$$w_{23} = \phi_2(x, T_2)\,e^{i\omega T_0} + W_2(x, T_0, T_2) + cc. \tag{32}$$

Substituting this solution into (20)–(23), we eliminate the terms producing secularities. Hence we deal with that part of the equation determining ϕ_i as follows:

$$\phi_1^{iv} - \omega^2\phi_1 = -2i\omega(A' + \mu A)Y_1 + (3/2)A^2\bar{A}\left[\int_0^\eta Y_1'^2\,dx + \int_\eta^1 Y_2'^2\,dx\right] Y_1'' + (1/2)F_1\,e^{i\sigma T_2}, \tag{33}$$

TABLE 2

The first five natural frequencies for different mass ratio, mass location and end conditions

Case I

α	η	ω_1	ω_2	ω_3	ω_4	ω_5
1	0·0	9·8695	39·4784	88·8264	157·9144	246·7413
	0·1	8·9962	29·8891	66·0691	127·2135	213·3439
	0·2	7·4541	26·9462	73·5140	149·3992	246·7413
	0·3	6·3946	29·7503	86·7293	143·2258	209·3172
	0·4	5·8468	35·2374	79·9788	132·6574	246·7413
	0·5	5·6795	39·4784	67·8883	157·9144	206·7901
10	0·0	9·8695	39·4785	88·8264	157·9144	246·7413
	0·1	5·3322	19·8959	59·0995	122·6556	210·0412
	0·2	3·2598	22·0545	70·7723	148·0797	246·7413
	0·3	2·5279	26·7706	86·1462	139·3226	204·6273
	0·4	2·2252	33·6806	77·2690	128·5117	246·7413
	0·5	2·1395	39·4785	62·4517	157·9144	200·6472

Case II

α	η	ω_1	ω_2	ω_3	ω_4	ω_5
1	0·0	2·4674	22·2066	61·6850	120·9032	199·8604
	0·1	2·4087	18·3454	45·1359	93·4431	167·2211
	0·2	2·2578	14·8086	46·3928	108·0103	196·6417
	0·3	2·0706	14·2145	54·4452	120·0471	166·6578
	0·4	1·8920	15·3836	61·6850	96·2916	188·1808
	0·5	1·7415	17·9539	53·0106	107·5473	181·7185
	0·6	1·6226	21·2279	45·5640	118·1939	173·8152
	0·7	1·5332	21·9816	50·9158	98·6861	193·0932
	0·8	1·4706	19·8790	61·6850	106·6180	165·0326
	0·9	1·4328	17·8328	55·9844	116·7804	198·9933
10	0·0	2·4674	22·2066	61·6850	120·9032	199·8604
	0·1	2·0037	10·0177	36·3461	87·8901	163·3744
	0·2	1·4140	8·9553	42·7450	105·9953	196·0784
	0·3	1·0683	10·0612	52·6275	119·7514	160·1237
	0·4	0·8662	12·2687	61·6850	90·5702	186·2925
	0·5	0·7395	15·7970	50·3531	104·6406	178·6633
	0·6	0·6560	20·5604	40·8105	117·5013	168·9948
	0·7	0·6000	21·8488	46·6505	94·8383	191·9832
	0·8	0·5634	19·0091	61·6850	101·5157	159·7266
	0·9	0·5421	16·5885	54·8768	116·0683	198·8297

Case III

α	η	ω_1	ω_2	ω_3	ω_4	ω_5
1	0·0	6·9049	31·8900	76·4168	140·6264	224·5502
	0·1	7·1089	34·0789	83·5771	155·3912	246·7413
	0·2	7·6615	38·3503	85·7404	130·1379	211·7200
	0·3	8·4912	37·8853	68·0983	141·5267	246·7413
	0·4	9·4084	30·6404	76·1398	154·1645	207·5299
	0·5	9·8696	27·6195	88·8265	127·5589	246·7413
10	0·0	5·7774	30·4219	74·8365	138·8365	222·8810
	0·1	6·0079	32·8614	82·6412	154·9477	246·7413
	0·2	6·6506	37·9387	84·3398	123·4099	207·8470
	0·3	7·6992	36·9612	62·5959	139·1055	246·7413
	0·4	9·0502	26·9754	73·3548	153·1530	201·8530
	0·5	9·8696	23·1098	88·8260	121·6874	246·7413

Table 2—(*continued overleaf*)

Table 2—(*continued*)

Case IV

α	η	ω_1	ω_2	ω_3	ω_4	ω_5
1	0·0	15·4182	49·9648	104·2482	178·2706	272·0322
	0·1	13·2773	36·9648	78·9377	146·4463	238·6747
	0·2	10·3964	35·8279	89·8535	172·3995	270·5268
	0·3	8·9482	41·1580	104·0726	153·4427	237·9214
	0·4	8·4780	48·5385	87·0356	158·8255	266·7995
	0·5	8·6977	47·2840	84·6891	172·7437	236·1355
	0·6	9·0600	38·6505	103·6283	145·8877	263·2084
	0·7	11·3683	33·0378	92·2403	178·0890	234·5798
	0·8	13·8203	33·2808	77·0176	153·7460	259·8318
	0·9	15·2752	45·5767	79·3377	133·4672	217·8576
10	0·0	15·4182	49·9648	104·2482	178·2706	272·0322
	0·1	6·7433	27·4534	72·7327	142·2724	235·5979
	0·2	4·1459	31·6794	87·4838	171·4502	270·1487
	0·3	3·3555	38·8358	104·0176	147·7781	234·1359
	0·4	3·1307	47·9812	82·5788	155·8378	265·7259
	0·5	3·2408	46·2242	80·2839	171·5340	231·1555
	0·6	3·7035	35·5186	103·4187	139·9891	261·8636
	0·7	4·7633	27·8717	90·1184	178·0410	228·1671
	0·8	7·2861	23·1321	72·2886	151·2088	258·4699
	0·9	13·6268	24·7908	60·5566	124·2400	212·1305

Case V

α	η	ω_1	ω_2	ω_3	ω_4	ω_5
1	0·0	2·9545	23·9392	63·4326	122·7165	201·7195
	0·1	3·0090	25·3661	69·0642	135·4291	223·2036
	0·2	3·1614	28·4668	74·0070	117·3647	187·0877
	0·3	3·4075	30·1129	58·3002	118·7904	220·4928
	0·4	3·7522	25·7223	59·1356	138·7920	196·5491
	0·5	4·1970	20·9093	71·6210	115·0728	216·3253
	0·6	4·7130	18·4833	70·3074	122·8417	195·9552
	0·7	5·1950	18·7343	57·8091	134·4440	208·7476
	0·8	5·4925	22·7446	50·6636	111·6425	203·5245
	0·9	5·5858	59·2073	61·9712	102·3233	172·2446
10	0·0	1·0756	22·5620	61·8705	121·1012	200·0584
	0·1	1·1036	24·1652	68·0335	134·8478	222·3767
	0·2	1·1831	27·8389	73·7213	110·9462	182·5687
	0·3	1·3190	30·0441	52·9205	115·6980	220·0772
	0·4	1·5302	23·4686	55·4268	138·7920	180·4132
	0·5	1·8570	17·0896	70·6208	110·4096	215·0827
	0·6	2·3796	13·1964	69·0978	119·2071	192·3353
	0·7	3·2543	11·0367	54·4383	133·5758	205·5496
	0·8	4·5913	9·8339	43·9142	108·0872	201·4753
	0·9	5·5150	19·3652	38·3650	89·3286	165·1867

$$\phi_2^{iv} - \omega^2\phi_2 = -2\mathrm{i}\omega(A' + \mu A)Y_2 + (3/2)A^2\bar{A}\left[\int_0^\eta Y_1'^2\,\mathrm{d}x + \int_\eta^1 Y_2'^2\,\mathrm{d}x\right]Y_2'' + (1/2)F_2\,\mathrm{e}^{i\sigma T_2}, \tag{34}$$

$$\phi_1 = \phi_2, \quad \phi_1' = \phi_2', \quad \phi_1'' = \phi_2'', \quad \phi_1''' - \phi_2''' + \alpha\omega^2\phi_1 - 2\alpha\mathrm{i}\omega A' Y_1 = 0 \qquad \text{at } x = \eta, \tag{35}$$

$$\phi_1 = \phi_1'' = 0 \quad \text{at } x = 0, \qquad \phi_2 = \phi_2'' = 0 \quad \text{at } x = 1. \tag{36}$$

In obtaining these equations, we substituted the first order solutions (24) and (25) into equations (20)–(23). We also assumed that the external excitation frequency is close to one of the natural frequencies of the system; that is,

$$\Omega = \omega + \epsilon^2 \sigma, \tag{37}$$

where σ is a detuning parameter of order 1. After some algebraic manipulations, one obtains the solvability condition for equations (33)–(36) as

$$2\mathrm{i}\omega(A' + \mu A) + (3/2)b^2 A^2 \bar{A} + 2\alpha \mathrm{i}\omega A' Y_1^2(\eta) - (1/2) f \,\mathrm{e}^{\mathrm{i}\sigma T_2} = 0, \tag{38}$$

TABLE 3

The non-linear frequency correction coefficients

		η	λ
Case I	$\alpha = 1$	0·1	1·6738
		0·3	1·1764
		0·5	1·0593
	$\alpha = 10$	0·1	0·8915
		0·3	0·4528
		0·5	0·3968
Case II	$\alpha = 1$	0·2	0·4224
		0·4	0·3531
		0·6	0·3038
		0·8	0·2753
	$\alpha = 10$	0·2	0·2552
		0·4	0·1591
		0·6	0·1226
		0·8	0·1052
Case III	$\alpha = 1$	0·1	0·8969
		0·3	1·3469
		0·5	0·00137
	$\alpha = 10$	0·1	0·4222
		0·3	0·9037
		0·5	0·000286
Case IV	$\alpha = 1$	0·2	1·1565
		0·4	0·9130
		0·6	0·9546
		0·8	1·2843
	$\alpha = 10$	0·2	0·4663
		0·4	0·3395
		0·6	0·3260
		0·8	0·4315
Case V	$\alpha = 1$	0·2	0·1847
		0·4	0·2035
		0·6	0·2437
		0·8	0·3046
	$\alpha = 10$	0·2	0·0698
		0·4	0·0801
		0·6	0·1003
		0·8	0·2015

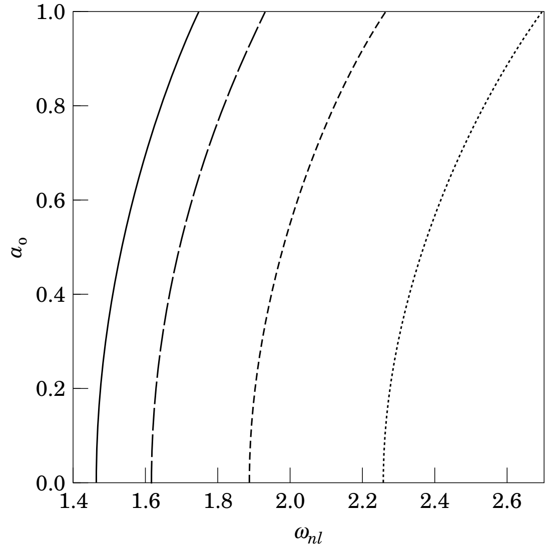

Figure 2. Non-linear frequency versus amplitude for different mass location values; first mode, Case II, $\alpha = 1$. - - - - , $\eta = 0{\cdot}2$; — — —, $\eta = 0{\cdot}4$; —— ——, $\eta = 0{\cdot}6$; ———, $\eta = 0{\cdot}8$.

where the equations are normalized by requiring

$$\int_0^\eta Y_1^2\,\mathrm{d}x + \int_\eta^1 Y_2^2\,\mathrm{d}x = 1 \tag{39}$$

and the coefficients are defined as follows:

$$b = \int_0^\eta Y_1'^2\,\mathrm{d}x + \int_\eta^1 Y_2'^2\,\mathrm{d}x, \qquad f = \int_0^\eta F_1 Y_1\,\mathrm{d}x + \int_\eta^1 F_2 Y_2\,\mathrm{d}x. \tag{40, 41}$$

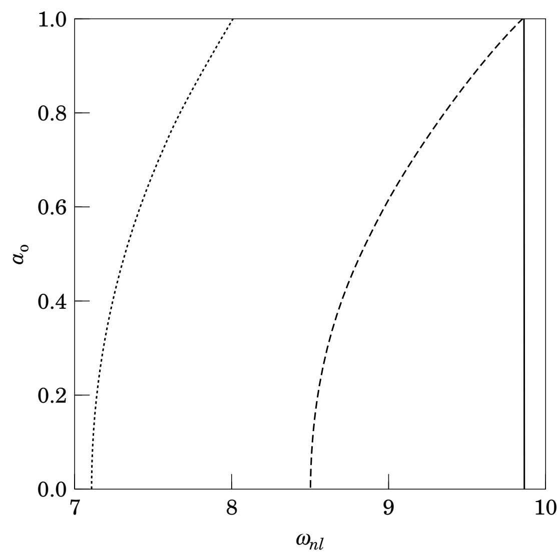

Figure 3. As Figure 2, but Case III. - - - - -, $\eta = 0{\cdot}1$; — — — —, $\eta = 0{\cdot}3$; ————, $\eta = 0{\cdot}5$.

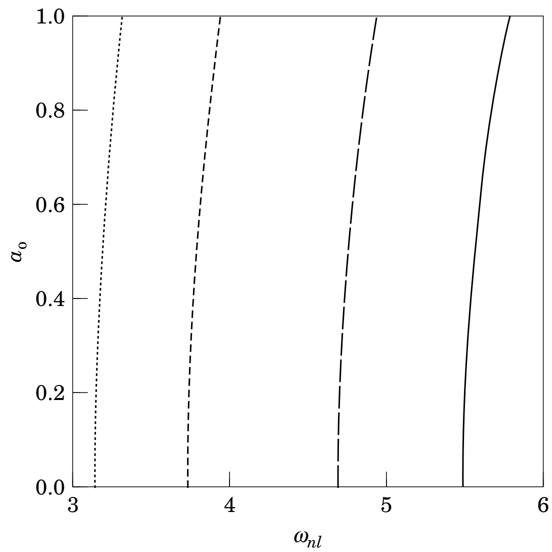

Figure 4. As Figure 2, but Case V. - - - - , $\eta = 0{\cdot}2$; – – –, $\eta = 0{\cdot}4$; — — —. $\eta = 0{\cdot}6$; ——, $\eta = 0{\cdot}8$.

Note that condition (38) is valid for all Cases I–V but, of course, the numerical values of b and $Y_1(\eta)$ differ for each case.

Equation (38) determines the modulations in the complex amplitudes. We use the polar form to calculate real amplitudes and phases:

$$A = (1/2)a(T_2)\,e^{i\theta(T_2)}. \tag{42}$$

Substituting equation (42) into equation (38), and separating real and imaginary parts, one finally obtains

$$\omega k a' = -\omega\mu a + 1/2f\sin\gamma, \qquad \omega k a\gamma' = \omega k a\sigma - 3/16b^2a^3 + 1/2f\cos\gamma, \quad (43, 44)$$

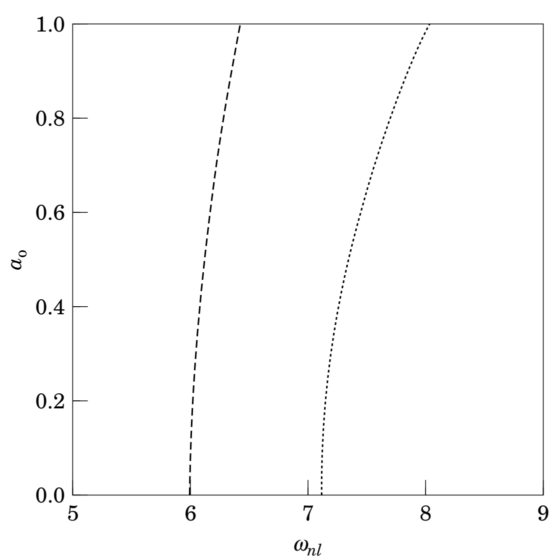

Figure 5. Non-linear frequency versus amplitude for different mass ratio values; first mode, Case III, $\eta = 0{\cdot}1$. - - - - , $\alpha = 1$; – – – – –, $\alpha = 10$.

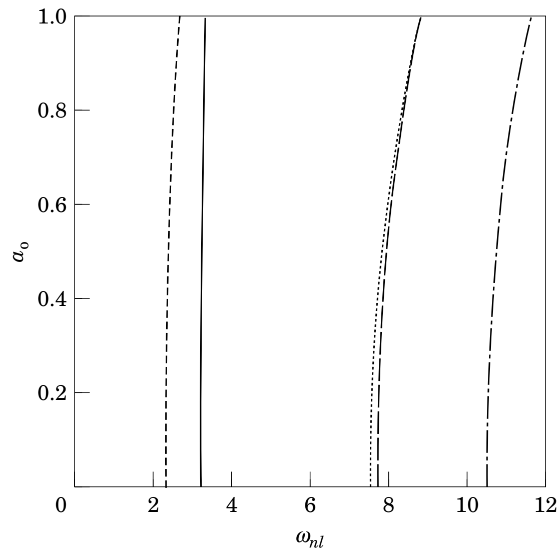

Figure 6. Non-linear frequency versus amplitude for different boundary conditions; first mode, $\alpha = 1$, $\eta = 0{\cdot}2$ · · · · , Case I; – – – – , Case II; — — —, Case III; — · — · , Case IV; ———, Case V.

where γ and k are defined by

$$\gamma = \sigma T_2 - \theta, \qquad k = 1 + \alpha Y_1^2(\eta). \tag{45}$$

To the first approximation, the beam deflections are given by

$$w_1 = \epsilon a \cos(\Omega t - \gamma) Y_1(x) + O(\epsilon^3), \qquad w_2 = \epsilon a \cos(\Omega t - \gamma) Y_2(x) + O(\epsilon^3), \quad (46, 47)$$

and the amplitudes and phases are governed by equations (43) and (44). Note that equations (43) and (44) allow for finding steady state as well as the transient solutions,

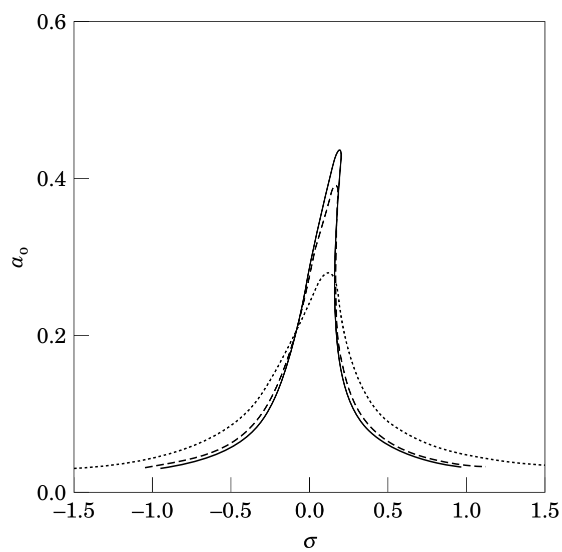

Figure 7. Frequency–response curves for different mass locations; first mode, Case I, $\alpha = 1$. - - - - - , $\eta = 0{\cdot}1$; – – – – , $\eta = 0{\cdot}3$, ——, $\eta = 0{\cdot}5$.

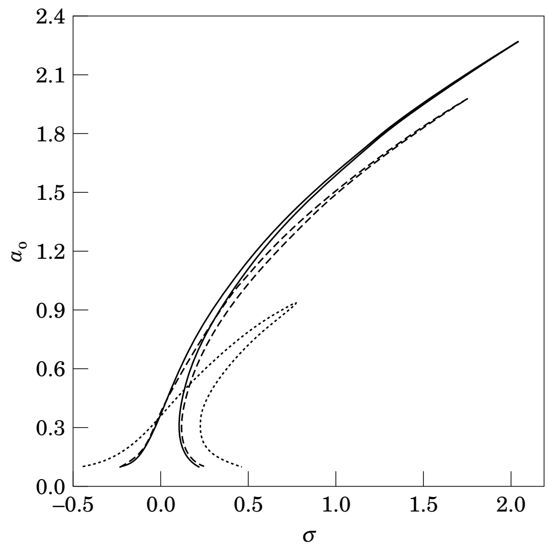

Figure 8. As Figure 7, but $\alpha = 10$.

an advantage of the method used over some other perturbation techniques, such as the harmonic balance or the Lindstedt–Poincaré technique.

4. NUMERICAL RESULTS

We first found the linear natural frequencies for each end conditions (Cases I–V) for various α and η values (Table 2). $\eta = 0$ corresponds to the case of beam without mass. Due to symmetry in Cases I and III, natural frequencies were calculated up to the mid-point. When α (the ratio of the concentrated mass to the beam mass) increases, regardless of the supporting conditions, the frequencies are lower. For Case I, due to symmetric support, $\eta = 0{\cdot}5$ becomes a node for the second frequency and one observes no change in the natural frequency as α becomes larger. In reference [8], for $\alpha = 1$ (ϕ in that reference) and $\eta = 0$, 0·1, 0·2, 0·3, 0·4 and 0·5 (λ in that reference), the fundamental frequency coefficients are given for an Euler–Bernoulli beam which, when squared, are exactly same as our results for Case I.

We next calculated the non-linear frequencies for free undamped vibrations. In equations (43) and (44), we took $\mu = f = \sigma = 0$ and obtained

$$a' = 0, \qquad \theta' = (3/16)(b^2/\omega k)\, a^2. \tag{48, 49}$$

From equation (48), $a = a_0$ (a constant) and hence the non-linear frequency is

$$\omega_{nl} = \omega + \theta' = \omega + \lambda a_0^2, \tag{50}$$

where

$$\lambda = (3/16)(b^2/\omega k). \tag{51}$$

To this order of approximation, then, the non-linear frequencies have a parabolic relation with the maximum amplitude of vibration. λ can be defined as the non-linear correction coefficient. For different α and η, the non-linear correction coefficients are listed in Table 3 for the first fundamental frequency corresponding to different cases. λ is a measure of the effect of stretching. The non-linearities are of hardening type. One sees from Table 3

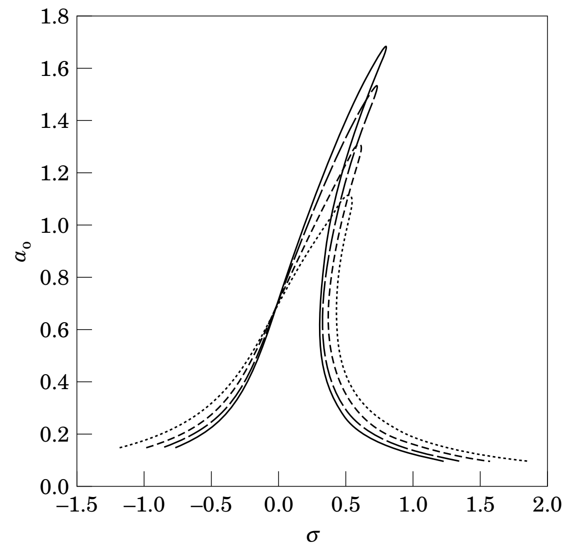

Figure 9. Frequency–response, curves for different mass locations; first mode, Case II, $\alpha = 1$. - - - - , $\eta = 0{\cdot}2$; – – –, $\eta = 0{\cdot}4$; — — — , $\eta = 0{\cdot}6$; ——, $\eta = 0{\cdot}8$.

that the effect of stretching decreases as α increases for all cases. For Cases I and IV, as η shifts to the mid-point, the effect of stretching decreases. For Case II, as η increases, there is a continuous decrease in the effect of stretching. On the other hand, the reverse is true for Case V. For Case III, the effect of stretching is very small for a centre-loaded beam. Some of the above conclusions are shown in Figures 2–6. Figure 2, for Case II, shows the variation of non-linear frequencies with amplitude. As η increases, the natural frequencies (ω_{nl} at $a_0 = 0$) and the effects of stretching decrease. For Case III, as the mass shifts to the centre, the natural frequencies increase. The stretching effects first increase and then decrease to a negligible value at the centre (Figure 3). For Case V, as η increases,

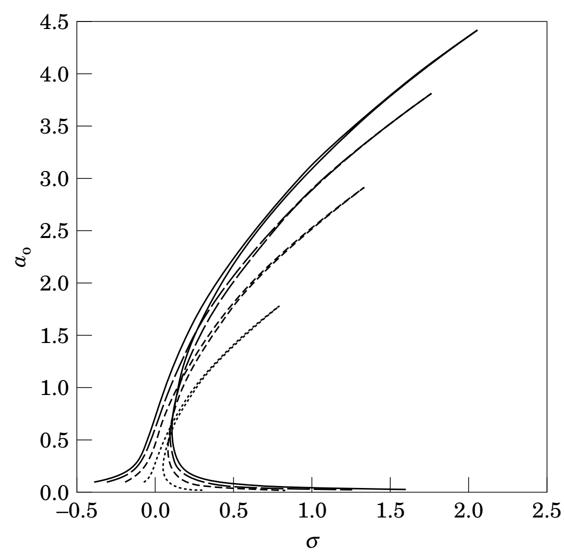

Figure 10. As Figure 9, but $\alpha = 10$.

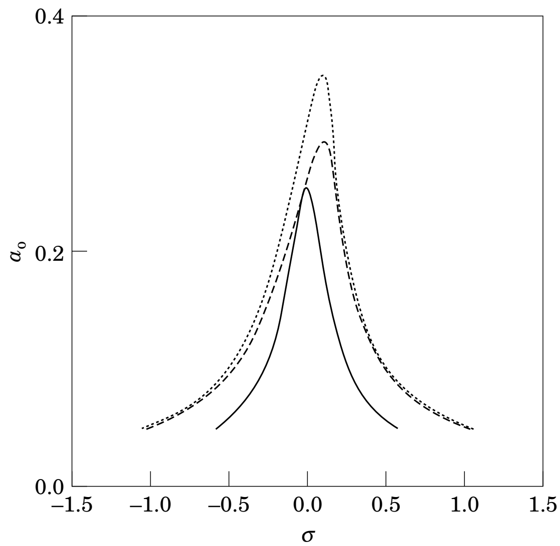

Figure 11. Frequency–response curves for different mass locations; first mode, Case III, $\alpha = 1$. - - - - - , $\eta = 0{\cdot}1$; – – – –, $\eta = 0{\cdot}3$; ———, $\eta = 0{\cdot}5$.

the natural frequencies and the stretching effects both increase (Figure 4). For all cases, the natural frequencies and the stretching effect decrease as α increases. An extreme example of this result is given in Figure 5. For $\eta = 0{\cdot}2$ and $\alpha = 1$, the non-linear frequencies for all cases are shown in Figure 6.

Before considering the forced vibrations, it is worth mentioning two of the recent studies on centre-loaded beams with different boundary conditions from the ones we have treated. In the work of Low *et al*. [21], a theoretical linear analysis was used and it was found that the results of experiments and the theory did not match well for beams of large slenderness ratio. In a later paper by the same authors [22], when stretching effects were included, the

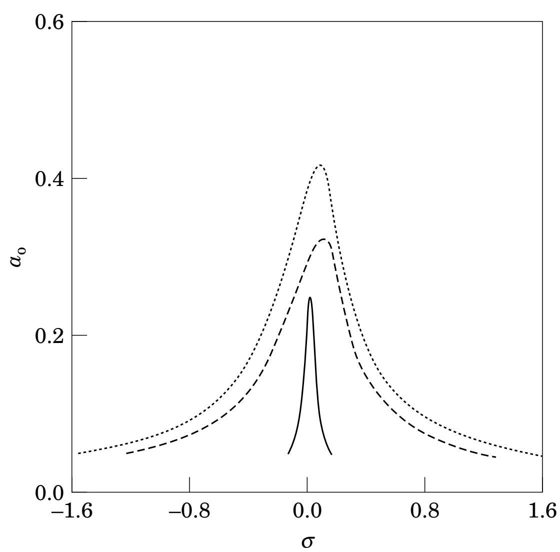

Figure 12. As Figure 11, but $\alpha = 10$.

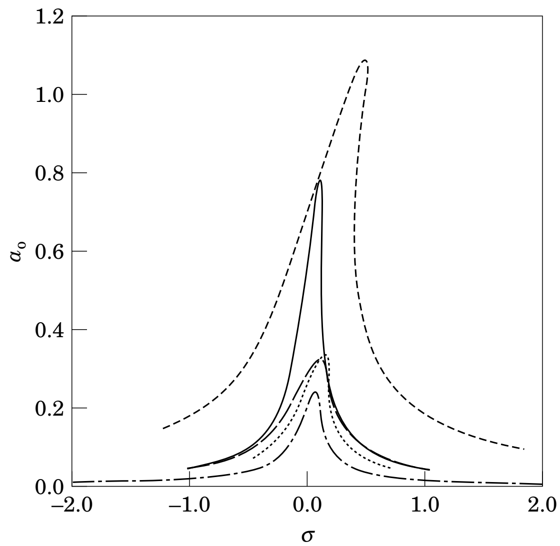

Figure 13. Frequency–response curves for different end conditions; first mode, $\alpha = 1$, $\eta = 0{\cdot}2$. - - - - , Case I; – – – –, Case II; — — — , Case III; — · — · — , Case IV; ———, Case V.

correlation between theory and experiments was much improved. They observed that the frequencies are higher for a beam under tensile effects due to the immovable boundary conditions, in agreement with what we have found. The tensile effects were calculated approximately using a Ritz procedure.

We now consider the case in which there is damping and external excitation. In equations (43) and (44), when the system reaches the steady state region, a' and γ' vanish and hence one obtains

$$\omega\mu a = \tfrac{1}{2} f \sin\gamma, \qquad -\omega k a\sigma + \tfrac{3}{16} b^2 a^3 = \tfrac{1}{2} f \cos\gamma. \tag{52, 53}$$

Squaring and adding both equations and solving for the detuning parameter σ yield

$$\sigma = \lambda a^2 \mp \sqrt{(\tilde{f}^2/4\omega^2 a^2) - \tilde{\mu}^2}, \tag{54}$$

where

$$\tilde{f} = f/k, \qquad \tilde{\mu} = \mu/k \tag{55}$$

and λ is defined in equation (51). The detuning parameter shows the nearness of the external excitation frequency to the natural frequency of the system. Several figures have been drawn by using equation (54). In Figure 7, the frequency–response curves for Case I are shown for different η values ($\alpha = 1$). The effect of stretching bends the curves to the right causing multi-valued regions of solution. This phenomena is the well-known jump phenomena. Note that the amplitudes are greater as one shifts to the middle for Case I. For this case, when α is increased, and other parameters kept constant, the multi-valued regions increase drastically, as shown in Figure 8. This same result can be seen from the comparison of Figures 9 and 10, which were drawn for Case II. However, the change is negligible for Case III, as shown in Figures 11 and 12. Case IV is similar to Cases I and II. In Figure 13, for fixed α and η ($\alpha = 1$, $\eta = 0{\cdot}2$) frequency response curves for Case I–V are shown on the same plot.

5. SUMMARY AND CONCLUSIONS

The non-linear response of a beam–mass system supported by five different end conditions has been investigated. The ends are immovable so that mid-plane stretching occurs during the vibrations, which produces non-linearities in the equations. Approximate solutions were sought by applying the method of multiple scales directly to the partial differential system. The first terms lead to the linear problem. Mode shapes and natural frequencies were calculated for different mass ratios, mass locations and end conditions. The second terms provide the non-linear corrections to the linear problem. Free and forced vibration with damping were investigated. Non-linear frequency–amplitude variation and frequency response curves have been presented.

As the mass ratio is increased, the natural and non-linear frequencies decrease. If the mass is located at a node, however, the frequencies may remain unchanged. One can observe that the stretching caused a non-linearity of the hardening type. When the mass is increased (α), the effect of stretching on the non-linear frequencies decreases for all cases. When the mass is shifted to the middle, the effect of stretching decreases for Cases I and IV. However, the situation is different for Cases II and V. When the mass is shifted from left to right, there is a continuous increase in stretching effects for Case V, whereas there is a continuous decrease for Case II. Negligible effects of stretching were found for the centre mass position of Case III. For forced and damped vibrations, since the non-linearity is of hardening type, the frequency–response curves are bent to the right, causing an increase in the multi-valued regions. When the mass ratio is increased, the multi-valued regions increase for Cases I, II and IV.

ACKNOWLEDGMENT

This work was supported by the Scientific and Technical Research Council of Turkey (TUBITAK) under project no. TBAG-1346.

REFERENCES

1. L. S. Srinath and Y. C. Das 1967 *Transaction of the American Society of Mechanical Engineers*, *Journal of Applied Mechanics*, *Series* **E**, 784–785. Vibrations of beams carrying mass.
2. R. P. Goel 1976 *Journal of Sound and Vibration* **47**, 9–14. Free vibrations of a beam–mass system with elastically restrained ends.
3. H. Saito and K. Otomi 1979 *Journal of Sound and Vibration* **62**, 257–266. Vibration and stability of elastically supported beams carrying an attached mass under axial and tangential loads.
4. J. H. Lau 1981 *Journal of Sound and Vibration* **78**, 154–157. Fundamental frequency of a constrained beam.
5. P. A. A. Laura, C. Filipich and V. H. Cortinez 1987 *Journal of Sound and Vibration* **117**, 459–465. Vibrations of beams and plates carrying concentrated masses.
6. C. N. Bapat and C. Bapat 1987 *Journal of Sound and Vibration* **112**, 177–182. Natural frequencies of a beam with non-classical boundary conditions and concentrated masses.
7. W. H. Liu and F. H. Yeh 1987 *Journal of Sound and Vibration* **117**, 555–570. Free vibration of a restrained-uniform beam with intermediate masses.
8. M. J. Maurizi and P. M. Belles 1991 *Journal of Sound and Vibration* **150**, 330–334. Natural frequencies of the beam–mass system: comparison of the two fundamental theories of beam vibrations.
9. S. Woinowsky-Krieger 1950 *Transactions of the American Society of Mechanical Engineers*, *Journal of Applied Mechanics* **17**, 35–36. The effect of an axial force on the vibration of hinged bars.
10. D. Burgreen 1951 *Transactions of the American Society of Mechanical Engineers*, *Journal of Applied Mechanics* **18**, 135–139. Free vibrations of pin-ended column with constant distance between pin ends.

11. A. V. SRINIVASAN 1965 *American Institute of Aeronautics and Astronautics Journal* **3**, 1951–1953. Large amplitude–free oscillations of beams and plates.
12. B. G. WRENN and J. MAYERS 1970 *American Institute of Aeronautics and Astronautics Journal* **8**, 1718–1720. Nonlinear beam vibration with variable axial boundary restraint.
13. A. H. NAYFEH and D. T. MOOK 1979. *Nonlinear Oscillations*. New York: John Wiley.
14. J. W. HOU and J. Z. YUAN 1988 *American Institute of Aeronautics and Astronautics Journal* **26**, 872–880. Calculation of eigenvalue and eigenvector derivatives for nonlinear beam vibrations.
15. P. H. MCDONALD 1991 *Computers and Structures* **40**, 1315–1320. Nonlinear dynamics of a beam.
16. M. A. DOKAINISH and R. KUMAR 1971 *Experimental Mechanics* **11**, 263–270. Experimental and theoretical analysis of the transverse vibrations of a beam having bilinear support.
17. M. PAKDEMIRLI and A. H. NAYFEH 1994 *Transactions of the American Society of Mechanical Engineers*, *Journal of Vibration and Acoustics* **166**, 433–438. Nonlinear vibrations of a beam–spring–mass system.
18. A. H. NAYFEH 1981 *Introduction to Perturbation Techniques*. New York: Wiley–Interscience.
19. M. PAKDEMIRLI and H. BOYACI 1995 *Journal of Sound and Vibration* **186**, 837–845. Comparison of direct-perturbation methods with discretization-perturbation methods for non-linear vibrations.
20. D. A. EVENSEN 1968 *American Institute of Aeronautics and Astronautics Journal* **6**, 370–372. Non-linear vibrations of beams with various boundary conditions.
21. K. H. LOW, T. M. LIN and G. B. CHAI 1993 *Computers and Structures* **48**, 1157–1162. Experimental and analytical investigations of vibration frequencies for centre-loaded beams.
22. G. B. CHAI, K. H. LOW and T. M. LIM 1995 *Journal of Sound and Vibration* **181**, 727–736. Tension effects on the natural frequencies of centre-loaded clamped beams.